









If modifying this program, a user should be aware of several awkward peculiarities of MATLAB; namely, that an object's data field can only be modified by that object's own methods, and not by other objects or methods, and that objects are not passed by reference. This, for example, means that to set a suspension's conductivity, one does not use `susp.med.sigma=.1`, or `setConductivity(susp,.1)`, but `susp=setConductivity(susp,.1)`.

### B. Best-Fit Regression

To find cell parameters from experimental data, a  $\chi^2$  minimization routine was developed. The user creates a suspension object (say, `susp`) with either default or custom static parameters. Then, given experimental data in the form of three vectors (`conductivities`, `crossoverFreqs`, and `errors`), and a vector of initial guesses for whichever parameters are to be varied (`guesses`, the command

```
crossoverfit(susp, conductivities, . . .
crossoverFreqs, errors, guesses)
```

will return a vector of best-fit parameters corresponding to the local  $\chi^2$  minimum. Essentially, the `crossoverfit` method provides a function to calculate  $\chi^2$  which is passed to the MATLAB function `fminsearch`, a high-speed built-in function capable of optimizing an unlimited number of parameters.

## IV. METHODS

### A. Cell Culture

Jurkat cells (human lymphoblastoid) were cultured at 37°C and 5%CO<sub>2</sub> in 25mL containers, and split 1:2 every two to three days. Culture medium was RPMI 1640 with 25mM HEPES and with L-Glutamine (Invitrogen) plus 10% FBS.

### B. Device Construction

The device used to measure crossover frequency was based on the “polynomial” electrode geometry, although it was not constructed precisely enough to exhibit the simple field gradients characteristic of that geometry. For construction, clear fast-cure epoxy (5104-3Z, Atacs Products) was spread as thinly as possible on a 3×1 inch, 1mm thick glass microscope slide. An equal size of aluminum foil was placed on top, and pressed down with several pounds of pressure overnight.

A pattern was cut into the aluminum foil using a fresh No. 10 scalpel blade. Epoxy was scratched away to whatever extent possible from the DEP region, and aluminum foil on one end of the slide was peeled back and twisted with 24 gauge stranded wire to make a clean electrical connection, since soldering to aluminum foil is inconsistent at best. The device is shown schematically in Fig. 5. For more information on the construction of this and other devices, the reader is referred to Appendix II.

### C. Experimental Setup

As in Figure 5, the DEP device was connected in parallel with a 10kΩ resistor, and in series with a 1μF electrolytic

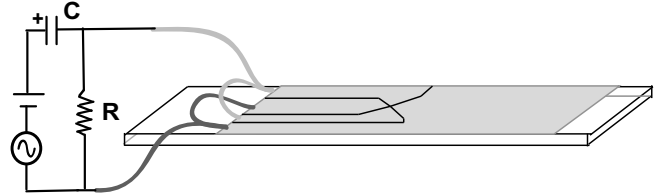


Fig. 5. Schematic of final DEP device. The electrical circuit served to prevent any DC bias or low-frequency signal from being applied to the DEP device. The lines on the device represent areas where aluminum was scraped away with a scalpel.  $R=10\text{k}\Omega$ ,  $C=1\mu\text{F}$ .

capacitor, to create a high-pass filter (corner frequency≈16Hz for attenuation of 1.5% at 100Hz). This setup protected the DEP device from the function generator's unpredictable DC bias, and from extremely low-frequency signals that were sometimes accidentally produced. Both of these, in the absence of the high-pass filter, caused damaging electrolysis in the DEP sample.

The function generator (Model F31, Interstate Electronic Corp) produced signals up to 3MHz, with an amplitude of up to 20V Peak-to-Peak. It was set to have at least a +7V DC offset to prevent damage to the electrolytic capacitor. The electronics were mounted on a standard breadboard (Jameco JE24) and connected by alligator clips and a BNC cable to the function generator, and to the DEP device by the 24 gauge stranded wire.

The DEP device was placed on the stage of a Zeiss Axiscop microscope capable of phase contrast. Images were captured on a Diagnostic Instruments CCD camera (Model #11.2 color mosaic), acquired in Spot Advanced 4.0.8 software, and processed in Adobe Photoshop 6.0.1. Phase contrast microscopy was performed as recommended by Murphy [18]: the microscope was adjusted for Köhler illumination, light was passed through a green filter, images were converted to grayscale, and levels were adjusted for clarity.

### D. Crossover Frequency Measurement

Crossover frequency measurements (frequency at which net DEP force is zero) were made with samples of varying conductivity. In an effort to ensure consistent timing and precise conductivity, the following procedure was performed separately for each sample:

5mL Jurkats were centrifuged 7 minutes at 1000 RPM, and the supernatant was removed. 5mL isotonic Sucrose/Dextrose (S/D) solution (8.5% sucrose, .3% dextrose w/v), kept at 37°C, was gently added and then poured off, without disturbing the cell pellet, to remove remaining RPMI. Cells were then resuspended in another 5mL S/D solution, vortexed, and centrifuged for seven more minutes. The supernatant was then poured off and cells were resuspended in .75mL S/D solution. 400μL of cell suspension was pipetted into a 1.5mL Micro Tube (Sarstedt) and mixed with a volume of isotonic saline solution (1%w/v NaCl). The conductivity of the suspension medium was found from an equation determined empirically using a Corning model 311 conductivity meter with temperature

compensation. Solutions ranged in conductivity from roughly 5 to 150 mS m<sup>-1</sup>, corresponding to S/D:1%NaCl ratios of 400:1 to 10:1.

As quickly as possible, 30 $\mu$ L of the suspension was pipetted onto the DEP device, covered with a 18×18mm No.1 cover slip, and observed using phase-contrast microscopy. The function generator was turned on, and cells were brought into regions of active DEP by applying a short 3MHz, 10V Peak-to-Peak signal. Several more such signals were applied, lowering the frequency by roughly half each time, until negative DEP was observed, and then raising the frequency in much smaller increments, until the crossover frequency was closely approached and DEP was no longer observed. This method of short bursts of moderate voltage prevented cells from lysing, as they sometimes do when DEP forces are quickly or drastically altered, or applied too strongly and for too long of a time. It also helps to prevent the suspension from heating up, which can alter the medium conductivity and hence the crossover frequency. Changing the frequency while keeping the voltage steady was found to be far less effective, and far more damaging to cells.

The generator voltage was then turned up to its maximum power of roughly 20 V Peak-to-Peak, and was finely adjusted to the frequency at which the majority of cells exhibited the least translational movement. At this frequency, cells would often rotate in place, which was a clue that the crossover frequency was being approached. This frequency was noted, along with its uncertainty, and the DEP device was thoroughly cleaned with 70% ethanol.

Moderate conductivities were tested initially, and then progressively higher and lower conductivities, until the crossover frequency became too difficult to accurately observe.

#### E. Fragment Creation and Quantification

Since our lab's eventual goal is to create a continuous-flow device to remove cell fragments, a method was devised to create and quantify cell fragments. The fragments were to be similar to those produced in cryopreservation, yet large enough to be detected.

Several methods of lysis were considered. Freeze/thaw lysis is a common technique [19], [20], and is sometimes used in combination with membrane-degrading detergents [21]. Hypotonic lysis, in which cells burst from osmotic pressure, has also been used on lymphoblasts alone [22] or in combination with detergents [23]. It sometimes involves complicated multi-stage lysis buffers [24] or subsequent homogenization [25], [26], but has even been performed with simple deionized water inside a microfluidic DEP device [27]. Furthermore, hypotonic lysis and freeze-thaw lysis are sometimes combined [28].

We decided against any method involving detergents or intense homogenization, since the electrical properties of cell components may be significantly altered, and since fragments may be different in size and shape from those created through cryopreservation. Freeze-thaw lysis was ultimately adopted due to its speed, effectiveness, and use in similar studies.

Our method of lysis and quantification was based loosely on that of Héault et al. [29], except that fluorescent labeling

of membranes was ultimately not performed. Briefly, two 5mL portions of cell culture ( $\approx 10^6$  cells mL<sup>-1</sup>) were centrifuged for 7 minutes at 1000 RPM, washed with PBS, centrifuged for another 7 minutes, and resuspended in 5mL PBS each. Eight 1mL full-strength portions and two 1mL half-strength (1:1 Suspension:PBS) portions were moved to 1.5mL Micro Tubes (Sarstedt). Of the full-strength portions, three were subjected to two freeze-thaw cycles (frozen in 80°C freezer for 25 minutes, thawed in 37°C water bath 10 minutes, two times), three were subjected to one freeze-thaw cycle, and two were kept as controls.

Quantification was performed using a FACScan 82665 flow cytometer (488nm laser, Becton-Dickinson) operated through CellQuest software (Becton-Dickinson). All channels were set to log, forward scatter was set to E-1, side scatter to 320, and forward scatter threshold to 10. No fluorescence channels were used, so compensation was unnecessary.

Each sample was vortexed at medium speed, and about 500 $\mu$ L was transferred to a flow tube (Model 2054, Falcon), which was again vortexed. Data were acquired for 30 seconds. Gates were drawn around both the cluster of cells and the large region of debris, as shown in Fig. 6, and were not moved between samples. Since an equal amount of fluid was processed in each sample, relative changes in debris and cell counts could be observed by comparing event counts between samples.

## V. RESULTS

Sizing of Jurkat cells on a hemocytometer using both fluorescent and phase contrast microscopy revealed a cell diameter of  $13 \pm 1.5 \mu\text{m}$  ( $n=160$ ).

A linear regression of conductivity vs. NaCl concentration (See Fig. 7) gave the conductivity of Sucrose/Dextrose-1%NaCl mixtures as

$$\sigma = 1527c + 2.36 \quad (10)$$

where c is NaCl concentration in %w/v and  $\sigma$  is conductivity in mS m<sup>-1</sup>. Conductivities were determined for 25°C, which is the temperature at which the DEP device operated.

Both negative (Fig. 8.a) and positive (Fig. 8.b) DEP were clearly observed for many different conductivities.

Conductivity and crossover data were also taken for PBS solutions to ensure than NaCl solutions did not produce anomalous results due to, for instance, pH. The data (not shown) was consistent with the NaCl data.

#### A. Crossover Frequencies and Best-Fit Regression

Crossover frequencies were measured at nine different conductivities. Several samples were tested repeatedly, and exhibited the same crossover frequency (within experimental uncertainty) for at least half an hour. The first data point was discarded since it was not consistent over time, and did not agree with data taken on another solution of identical conductivity. The discrepancy is thought to be due to small amounts of detergent left over from cleaning the device, and emphasizes the need for cleanliness when working with low-conductivity solutions.

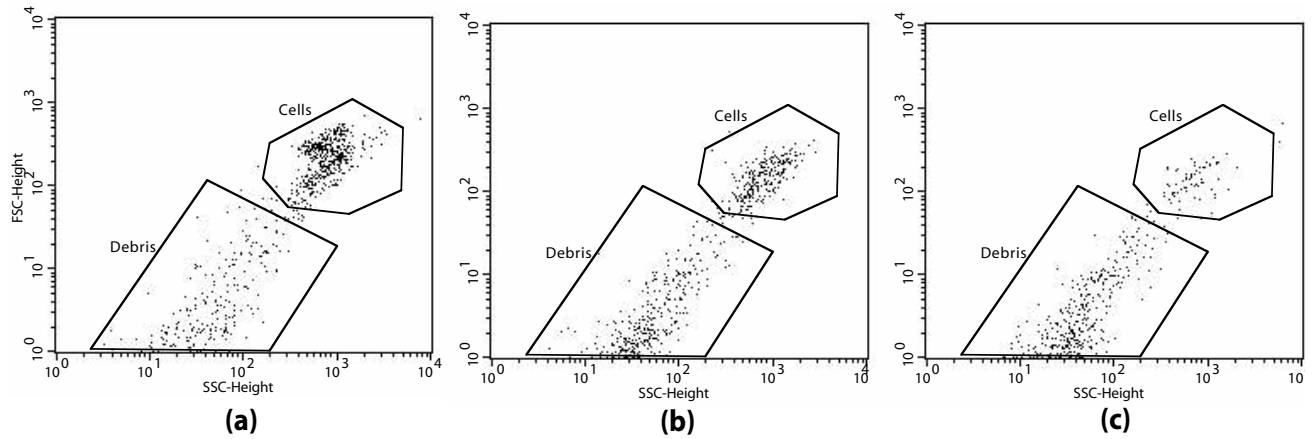


Fig. 6. Dotplots of flow cytometer events, showing forward scatter vs. side scatter. From left to right: a typical unlysed sample (a), a once freeze-thawed sample (b), and a twice freeze-thawed sample (c). Note the clear, distinguishable groupings of cells and debris, and the noticeable decrease in cell events following each freeze-thaw cycle.

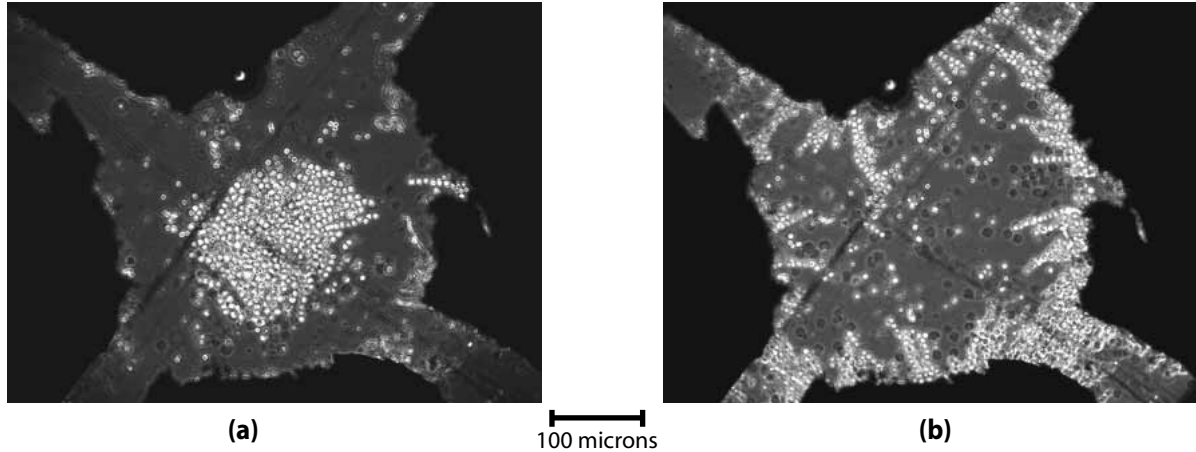


Fig. 8. Images after several minutes of negative (a) and positive (b) DEP. Medium conductivity was  $18 \text{ mS m}^{-1}$ . Crossover frequency was about 90kHz.

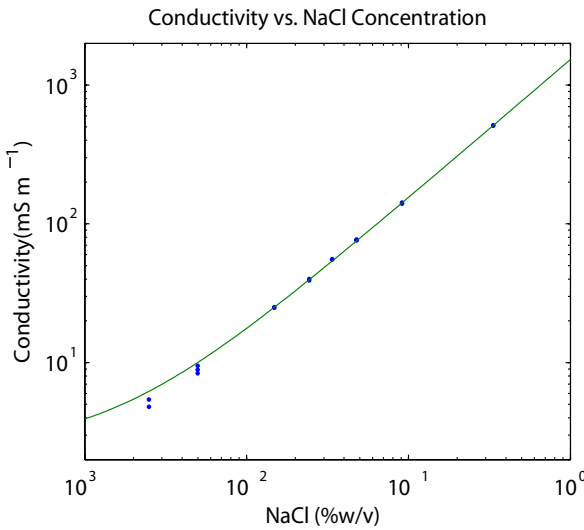


Fig. 7. Conductivity of a solution formed by mixing a 1%NaCl solution with a 8.5%Sucrose/.3%Dextrose solution. Experimental data and the linear regression (10). The discrepancy between the regression and the low values is due to the small conductivity even when no NaCl is present. Error is  $\pm 2\%$ .

Crossover and conductivity data was then processed and plotted in MATLAB. A best-fit regression using the single-shell model (described previously) was then performed. As discussed in Appendix I, membrane permittivity was the only parameter fitted and, as noted by Jones [30], is the most significant unknown electrical parameter at intermediate frequencies in low-conductivity solutions.

The starting value for membrane permittivity, as well as the assumed values for membrane conductivity, cytoplasmic permittivity and conductivity, and membrane thickness, were taken from the literature [10], [31]–[33]. Experimental data, as well as initial and best-fit predictions, are shown in Fig. 9.  $\chi^2$  per degree of freedom was reduced from 60 to 10 by the fitting algorithm.

DEP, as usual, was weak and inconsistent at higher conductivities, and thus had a great uncertainty. Likewise, at very low low conductivities, the conductivity itself was in question due to both contaminants potentially left on the DEP device and ion leakage through the cells' membranes [34], [35].

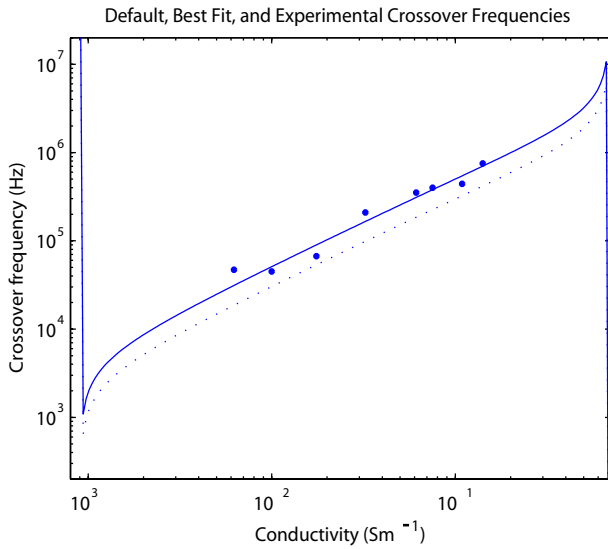


Fig. 9. Graph of crossover frequencies as a function of conductivity. Dotted line represents default cell parameters ( $\chi^2/\text{DoF} \approx 60$ ), while the solid line represents best-fit parameters ( $\chi^2/\text{DoF} \approx 10$ ). Dots are experimental data. Parameters are in Table I.

TABLE I  
REGRESSION PARAMETERS AND RESULTS

Parameter	Starting Value	Best Fit Value
cell radius	$6.5 \mu\text{m}$	-
membrane thickness	$4.5 \text{ nm}$	-
cytoplasmic relative permittivity	65	-
membrane relative permittivity	5.6	3.3
cytoplasmic conductivity	$0.7 \text{ S m}^{-1}$	-
membrane conductivity	$6.3 \times 10^{-7} \text{ S m}^{-1}$	-

### B. Cell Lysis

In the CellQuest software, regions containing cell events were easily distinguished from those containing debris, as shown previously in Fig. 6. Furthermore, cell events decreased from the original suspension to the single- and double-lysed samples, as debris events increased, in both the forward and side scatter channels, as can be seen in Fig. 10.

Cell, debris, and total event counts are summarized in Table II as the mean of  $n$  samples  $\pm$  the standard deviation. In unlysed suspensions, cell count is consistent within a few percent. The first freeze-thaw cycle reduces the cell count by roughly 60% while doubling the debris count, and the second cycle reduces the cell count by another 70% but actually lowers the debris count by about a third. Furthermore, the total event count after two freeze-thaw cycles is roughly half of the initial count. This is most likely due to aggregations of cells and debris, which were observed primarily in the twice-cycled samples. Aggregation has previously been observed to decrease with decreasing cell concentration, and might also be lessened by the use of DNase, but this was not

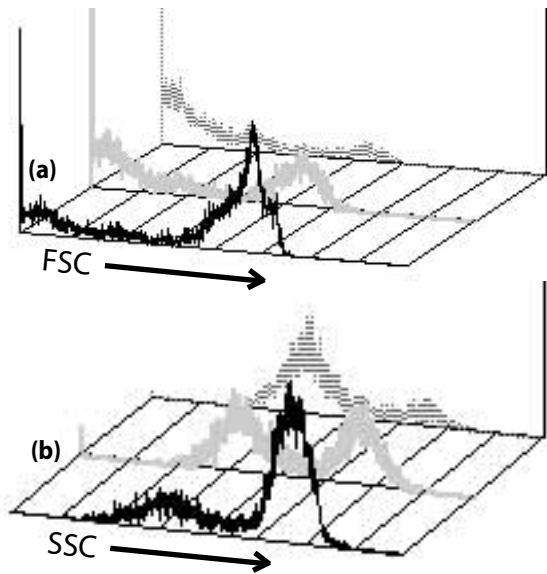


Fig. 10. Histograms of forward scatter (a) and side scatter (b) events. From front to back are unlysed cells (black line), once freeze-thawed cells (light gray line), and twice freeze-thawed cells (dark gray line). Note in both plots the decrease in cells and the increase in debris after each freeze-thaw cycle. Region statistics are summarized in Table II.

TABLE II  
EVENT COUNTS IN THOUSANDS

Type	$n$	Cells	Debris	Total
Full strength suspension	3	$9.03 \pm 0.08$	$4.1 \pm 1$	$14.0 \pm 1$
Half strength suspension	3	$4.39 \pm 0.04$	$1.42 \pm 0.07$	$6.16 \pm 0.05$
Single freeze/thaw cycle	6	$3.9 \pm .3$	$9.0 \pm 2.7$	$15 \pm 3$
Double freeze/thaw cycle	6	$1.1 \pm 1$	$6.7 \pm 3$	$8.8 \pm 5$
Supernatant	3	$.27 \pm 0.02$	$46 \pm 2$	$54 \pm 3$

tested. Héault observed aggregation in samples with initial cell concentrations greater than  $10^6 \text{ cells/ml}^{-1}$  [29].

Perhaps most surprising, though, is the enormous amount of debris in the supernatant that was collected before the first PBS wash—enough debris that the supernatant may be an even better source of cell fragments than freeze-thaw lysing. This factor may have complicated several of our earlier studies, and underscores the need to wash cells several times before performing this type of analysis.

## VI. DISCUSSION AND RECOMMENDATIONS

### A. Validity of Models

The single-shell model seemed to be fully sufficient for modeling the DEP response of Jurkat cells, and can be expected to accurately model stem cells once their electrical properties are determined. The only discrepancy encountered so far is the low DEP forces at high conductivities.

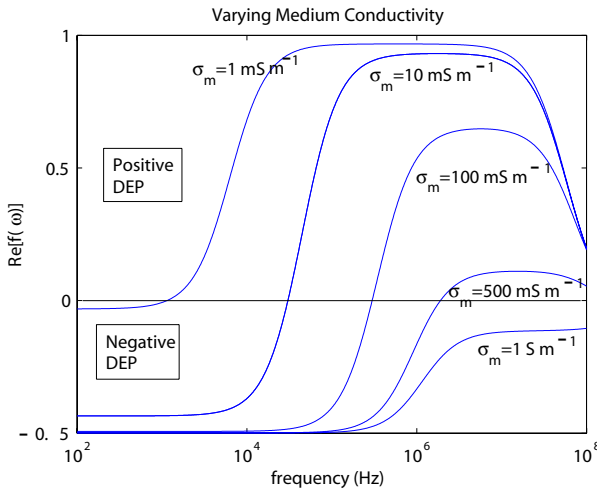


Fig. 11. Predicted  $\text{Re}[f(\omega)]$  vs. Frequency graphs for several Jurkat cells in several different medium conductivities.

For instance, plots of  $\text{Re}[f(\omega)]$  vs. Frequency (see Fig. 11) indicate that cells should experience the strongest possible negative DEP force at low frequencies and high medium conductivities, since  $\text{Re}[f(\omega)]$  is at its lowest possible value. Yet, while negative DEP is observed in these cases, it is very weak. Furthermore, it does not seem likely that the electric field is altered by high-conductivity media, since the line integral from one electrode to another is a function only of the voltage difference, and should not change as long as the medium is homogenous. Other possible explanations include a rapid oxidation of the aluminum electrodes due to the increased flow of ions, so that the bulk of the voltage drop happens across an insulating aluminum oxide layer, or a possible lowering of impedance across the DEP device which may result in the voltage drop happening across the capacitor. Still, at low to medium conductivities, the model appears to be excellent. *Note: see Appendix III for recent observations on conductivity, including the probable reason for the weak DEP observed at high conductivities.*

The cell fragment model, however, leaves much to be desired, and at the same time may be difficult to improve. Fragments could be modeled as pancake-like dielectric ellipsoids using equations covered by Jones [30], but this would still not account for the overwhelming diversity in fragments. Ultimately, an empirically determined relationship between field frequency and fragment elution might be most useful.

### B. Device construction

The clear choice for electrode design seems to be the interdigitated geometry due to the relative ease of construction, the small possible electrode widths and gaps, and the simple equations available to describe its field.

The spacing between electrodes is a trade-off between high field gradients and high DEP forces (small spacing), and longer reach of the DEP force (large spacing). For a given levitation height, the spacing which produces the largest DEP force can be found by setting the partial with respect to the

electrode spacing  $d$  of (6) equal to zero. Solving for  $d$ , we find:

$$0 = e^{-\frac{\pi h}{d}} (\pi h d^{-5} - 3d^{-4}) \quad (11)$$

$$d = \frac{\pi}{3} h \approx 1.05h \quad (12)$$

so that, to levitate particles at a height of  $20\mu\text{m}$  with the lowest possible voltage, the electrode width and gap should be roughly  $21\mu\text{m}$ . One complicating factor, though, is that joule heating in the solution is proportional to  $\sigma|E|^2$ , so that for large voltages and high conductivities, heating can become very significant [36]. However, small electrodes can effect large field gradients with small field magnitudes, and thus produce large DEP forces without excessive heating.

Several overall designs seem to have potential. First, if wash fluid enters on the top and the cell suspension on the bottom, a field could be applied so that the cells experience a slight negative DEP force, and are hence levitated perhaps  $10\mu\text{m}$  above the electrodes. Debris, meanwhile, would ideally feel either a strong positive or negative DEP force, and would be trapped on the electrodes, or repelled into the wash stream. Unfortunately, DEP may be unable to gently levitate cells while getting rid of fragments, especially those that would feel negative DEP, since DEP force scales with particle size and drops quickly with height above the electrodes.

Another possible design could involve, for instance, the cell suspension entering above the wash stream as in Fig. 12. Widely-spaced electrodes on the top of the chamber could very quickly repel cells down to the bottom. Narrowly-spaced electrodes at the lower surface could then prevent cells from touching the bottom and becoming damaged or stuck, since they would create large DEP forces, but only at short distances. Cell debris and DMSO, which ideally would be relatively unaffected by DEP, sedimentation, or diffusion forces (due to the small possible device length and, hence, short time scales), would simply remain near the top of the flow stream and be washed out. Two successive washes could probably also remove most of the DMSO from within the cells. Such a design might enable rapid processing, even up to the limits of laminar flow, since it would not depend on diffusion to remove DMSO. Since studies by Docoslis have shown that DEP forces on cellular debris in high-conductivity solutions may be minimal, but that negative DEP forces on live cells in those solutions are significant [37], [38], a device such as the one just described, which does not rely on dielectrophoresis of cell fragments or dead cells, may be the only viable option. Furthermore, a diffusive DMSO removal device, in series with the just-described dielectrophoretic device, might be a potent combination.

### C. Conductivity

Conductivity has proved to be a significant obstacle to us, but there are several promising solutions. First, platinum electrodes may alleviate the problem in the unlikely case that the aluminum was being oxidized. Second, as mentioned earlier, conductivity decreases with temperature. DEP processing of cells immediately following thawing, at which point the cells

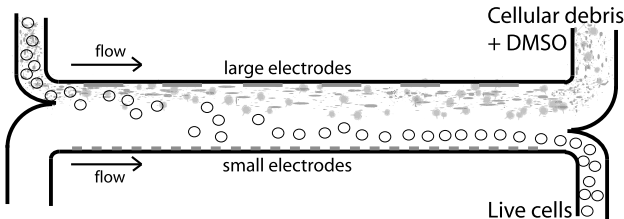


Fig. 12. An alternative design, employing exclusively negative DEP, and relying on neither diffusion nor DEP of dead cells or cell fragments. The top electrode array pushes cells towards the more closely spaced bottom array, which levitates them just above the lower surface.

would be near or even slightly below 0°C, might both increase DEP effectiveness and decrease the effects of DMSO toxicity.

The effects of a temperature decrease are not fully understood at this time, but it seems probable that permittivity will be affected to a much lesser degree than conductivity, and that the dielectrophoretic response of a given suspension will indeed change significantly with temperature.

#### D. Future experiments

1) *Levitation height:* Although crossover frequency experiments can yield important information about several electrical parameters, they leave significant uncertainty about the value of  $\text{Re}[f(\omega)]$ . Levitation height experiments, on the other hand, can find  $\text{Re}[f(\omega)]$  for any combination of parameters, so long as it is sufficiently negative to enable levitation.

If fields of varying frequency are applied to different cell suspensions, the height of levitation (sometimes measured by focusing a high-powered microscope on a cell) can be used to back out  $\text{Re}[f(\omega)]$  by setting the DEP force equal to the sedimentation force in (3). Best-fit regressions can then be performed.

2) *Cell and cell fragment elution using flow cytometry:* Since cell fragments are difficult to observe in a microscope, and since their sedimentation force would be extremely difficult to calculate, levitation height experiments are less applicable. Still, elution experiments can be performed in which output from a device is piped into a Coulter counter or into the needle of a flow cytometer [1], [5].

One possible experiment is measuring cell and fragment elution from a DEP device as a function of frequency. By characterizing the size and type (membrane, non-membrane, etc.) of fragments, their crossover frequencies can be determined. Furthermore, a single pulse of cell suspension injected into the device will undergo field-flow-fractionation. Thus, plots of stream contents as a function of time can reveal information about levitation heights.

## VII. CONCLUSION

Dielectrophoresis of viable cells was characterized and demonstrated, and progress was made towards understanding and being able to effectively study the dielectrophoresis of cell fragments. A practical and effective method of fragment creation and quantification was established.

## APPENDIX I SENSITIVITY ANALYSIS

Sensitivity analysis was performed on both the Crossover Frequency vs. Medium Conductivity graphs (Fig. 13) and the  $\text{Re}[f(\omega)]$  vs. Frequency graphs (Fig. 14).

The former case is particularly important because Crossover Frequency vs. Medium Conductivity is used by both our group and other groups to determine cells' physical characteristics. As can be seen in Figure 13, each parameter affects the graph in a different way. Cell radius and membrane thickness move the left corner of the graph horizontally, effectively shifting the linear portion vertically. Membrane conductivity moves the left corner diagonally, and so does not substantially affect the linear portion. Cytoplasmic permittivity and Cytoplasmic conductivity primarily alter the right corner of the graph. Membrane permittivity shifts the entire graph vertically.

Since we have thus far only been able to collect data on the linear portion of the graph, a best-fit regression will yield no information about cytoplasmic permittivity, cytoplasmic conductivity, or membrane conductivity. Furthermore, since the angle of the line does not change, a best-fit regression on the linear portion of the graph can alter only one parameter: the vertical position of the line.

Thus, we are left with three parameters that will all produce an equally good fit: membrane thickness, membrane permittivity, and cell radius. Membrane thickness has been accurately established by methods such as x-ray diffraction, which are far more accurate than dielectrophoretic modeling [33]. Furthermore, cell radius has been established rather accurately by cell sizing.

Therefore, it seems prudent to fit the curve using membrane permittivity as the only fitting parameter. Low-frequency measurements made using an extremely pure, low-conductivity medium, and high-frequency measurements using very small electrode spacings (and hence high field gradients) could cast light on the other parameters, as could fitting of  $\text{Re}[f(\omega)]$  vs. frequency data by measuring DEP levitation height. Accurately determining these other parameters would be important to modeling since, while some of them have negligible effects on the crossover frequency at a given conductivity, they can have a marked effect on the DEP forces (See Fig. 14). Currently, though, we must rely on published data to estimate those properties.

## APPENDIX II DEP DEVICES

Over the course of the project, over twenty DEP devices were designed, built, and tested. Many of these are pictured in Fig. 15. Two main methods of construction were used.

The first method of construction used 30-gauge ( $250\mu\text{m}$  dia.) magnet wire, which has an extremely thin layer of insulation around it. The wire was attached to the microscope slide using super glue or fast-cure epoxy. If required, the surface of the wires and super glue or epoxy could be scratched away with a scalpel, revealing a pattern of electrodes in whatever shape the wire was placed on the slide. In Fig. 15, devices (b), (c), (h), (i), and (j) use this mode of construction.

Unfortunately, as is especially evident in **(i)**, the epoxy and super glue were not especially hard and became very rough and dirty when scratched away, making cell observation difficult.

The second method of construction used either platinum foil (.025mm thick, Aldrich) or more frequently, aluminum foil. First, the foil was attached to a microscope slide by a thin layer of fast-cure epoxy or, sometimes, super glue. Conventional epoxy did not perform better than fast-cure, and fast-cure performed much better than super glue for affixing aluminum foil. Second, a pattern was cut into the foil using a fresh scalpel, and unwanted foil was gently pulled away, leaving potentially detailed electrode designs on the slide. Device **(a)**, which was the most successful device, and devices **(d)-(g)**, were constructed by this method. Ultimately, aluminum foil proved to be much softer and easier to use than platinum foil, and did not exhibit any noticeable corrosion problems.

Finally, several devices deserve further explanation. Device **(j)** is a pin-and-plate design that uses magnet wire for both the pin and the plate. Device **(k)** is also a pin-and-plate design, but uses platinum foil for the pin, and a fragment of a scalpel blade for the plate. Device **(l)** uses two aluminum electrodes (not pictured) to apply a voltage across two reservoirs, separated by two shards of broken cover-plate. The opening between the two shards is exceedingly small, ideally creating a large voltage drop, to be used in “electrodeless” DEP. Unfortunately, small amounts of fluid were able to flow above and below the shards, preventing DEP from taking place.

### APPENDIX III

#### ADDENDUM: UNEXPECTEDLY LOW DEVICE IMPEDANCE

An important observation was made, although unfortunately time does not permit further investigation, or proper incorporation into the report. DEP device voltage was recorded as a function of frequency using the Fluke 77 Series II multimeter. Results are plotted in Figure 16. First, it was observed that even with the device running dry, the filter response was significantly different than was predicted:

$$\left| \frac{V_{DEP}}{V_{applied}} \right| = \left| \frac{R}{1 + \frac{1}{j\omega C}} \right| \quad (13)$$

but that using a value of  $C=100nF$  matched the observed response almost exactly. So, it appears that the capacitor is  $\frac{1}{10}$  of what we had thought, although it shouldn't make a huge difference.

Furthermore, trial-and-error curve fitting revealed that the impedance of the DEP device with the 10%PBS solution, which has a conductivity of  $\approx 150mS m^{-1}$ , is roughly  $700 \pm 200\Omega$ , and that the impedance is frequency-dependent, since there was no resistance that resulted in convincing agreement along the entire curve. Similar analysis showed the impedance of pure PBS to be  $200 \pm 75\Omega$ . There is a good chance that the device, when filled with fluid, has a large capacitive component.

One avenue that may be worth pursuing is coating electrodes with an extremely thin layer of insulating dielectric material to prevent electrolysis. For instance, Jones [39], Wong [40], and undoubtedly many others have used this technique, though

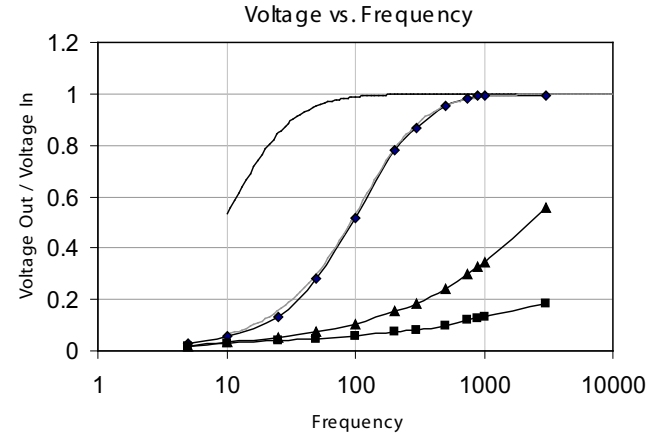


Fig. 16. Plots of DEP device voltage divided by supplied voltage. The black line is expected values for  $C=1\mu F$ , and the grey line is expected values for  $C=100nF$ . Diamonds are actual values of the DEP device running dry, triangles are with 10% PBS, and squares are with pure PBS.

their work was with much smaller amounts of fluid. Such a system, however, may require comparatively high frequencies to overcome the impedance of the dielectric layer.

It seems probable that negative DEP *will* be observed strongly at low frequencies, as the models predict. Unfortunately, the convection currents and electrolysis already observed at high conductivities will be amplified many times if the high-pass filter is configured to allow sufficient current through it. Extremely narrow electrodes using low voltages would provide sufficient DEP forces without heating, but the forces would not reach very far into the fluid.

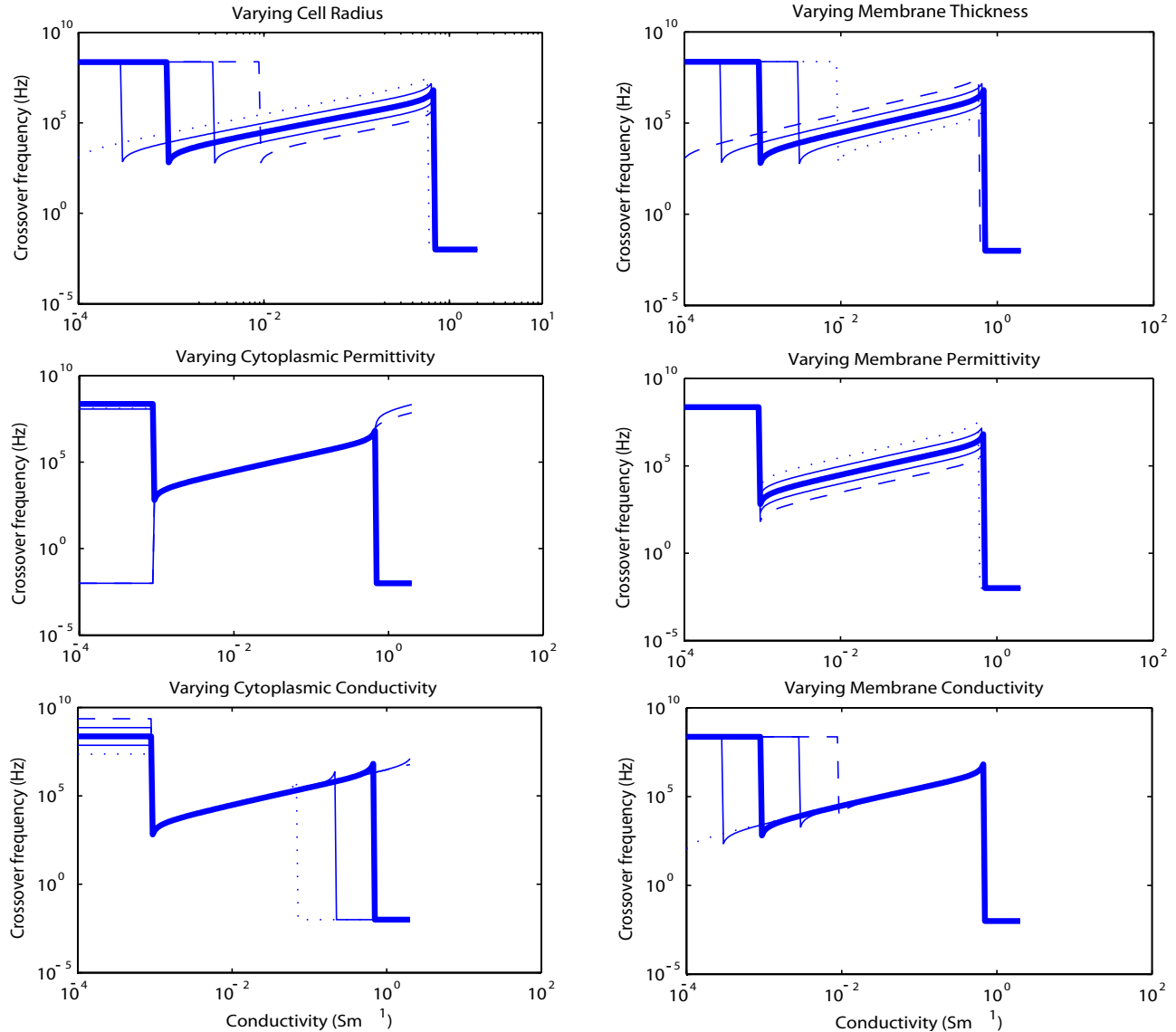


Fig. 13. Crossover Frequency vs. Conductivity graphs from sensitivity analysis of the six cell parameters. In each graph, the indicated parameter was plotted at the default value (thick line), and at the default value times  $10^{-1}$  (dotted line),  $10^{-5}$ ,  $10^5$ , and  $10^1$  (dashed line). Note that several parameters have no effect on the linear portion of the graph on which our data lies.

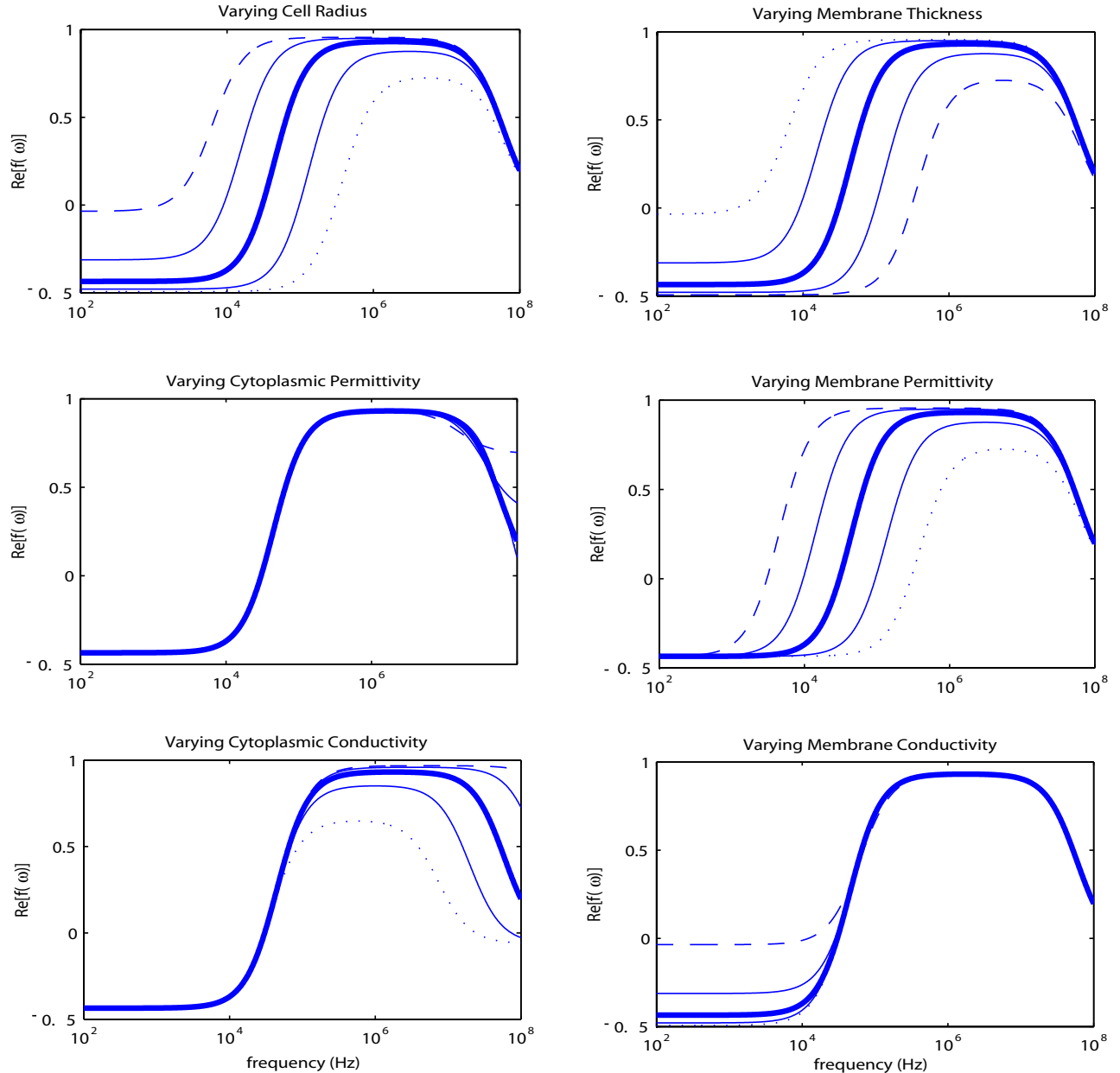


Fig. 14.  $\text{Re}[f(\omega)]$  vs. Frequency graphs from sensitivity analysis of the six cell parameters. Medium conductivity is  $10 \text{ mS m}^{-1}$ . In each graph, the indicated parameter was plotted at the default value (thick line), and at the default value times  $10^{-1}$  (dotted line),  $10^{-5}$ ,  $10^{-5}$ , and  $10^1$  (dashed line). Note that several parameters (such as cytoplasmic conductivity and membrane conductivity) have a significant effect on these graphs, but not on those of Fig. 13. Note also that  $\text{Re}[f(\omega)]$  is proportional to DEP force and is thus important to determine accurately.

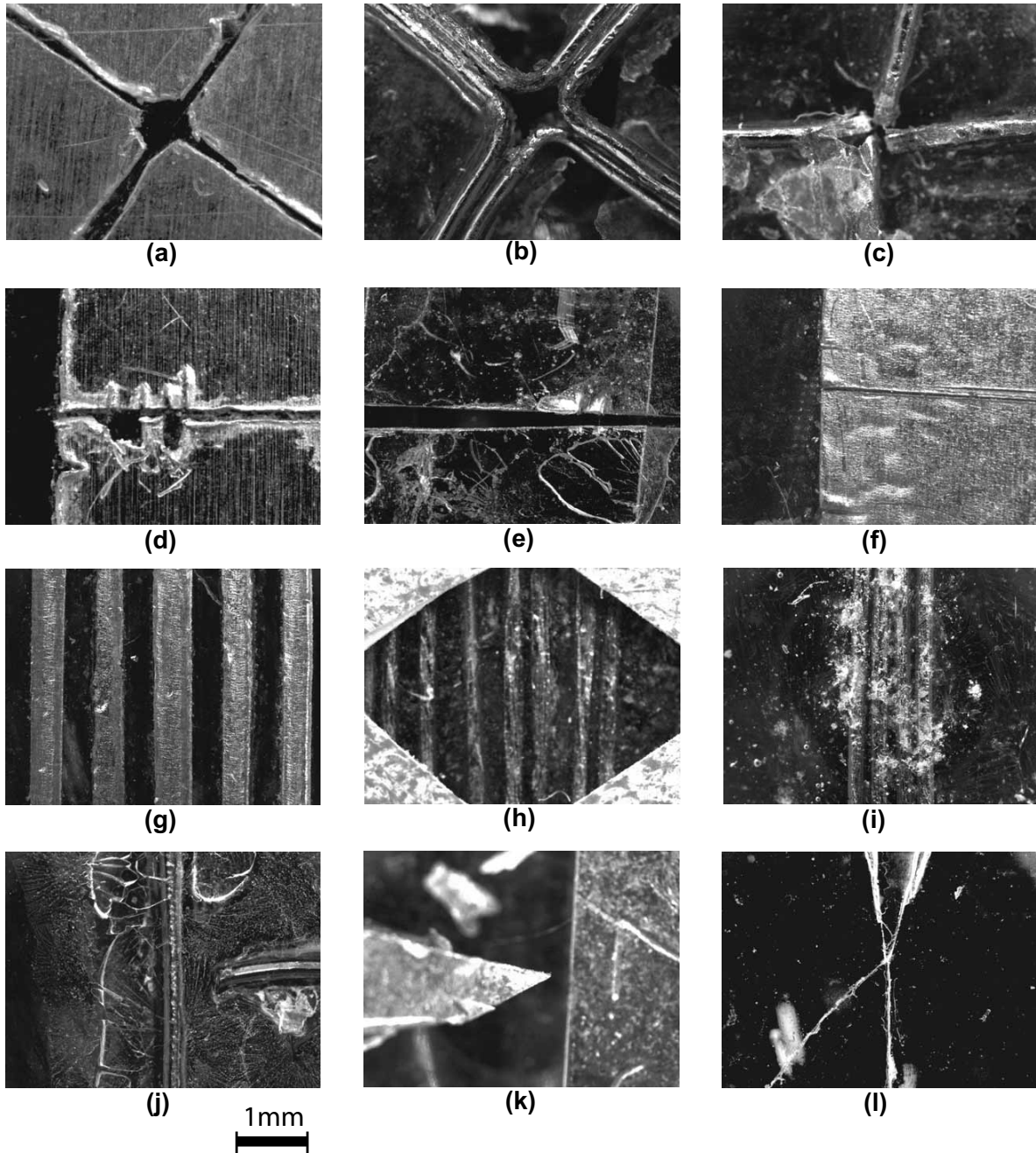


Fig. 15. Several DEP Devices. Devices **(a-c)** are based on the “polynomial” electrode geometry, **(d-f)** are designed to behave somewhat like an “intercastellated” geometry (with only two electrodes), **(g-i)** are designed to mimic the “interdigitated” geometry, and devices **(j)** and **(k)** are “pin and plate” designs. Device **(l)** is designed to perform electrodeless DEP (EDEP) [6], [14], [15], and the two electrodes are positioned outside the field of view.

## APPENDIX IV MATLAB CODE

The author would like to apologize for writing object-oriented code in MATLAB; he didn't realize how ugly it would get until he was already too far into it.

### A. Typical commands

To plot the Clausius-Mossotti factor as a function of frequency, for a Jurkat cell in 150mS/m water:

```
>> s=suspension('Jurkat in 150mS/m Water', jurkat, setConductivity(medium,.15));
>> plotK(s,2,8)
```

To fit for membrane permittivity, given a suspension *s*, column vectors of crossover frequencies *fxos*, conductivities *conds*, nacl percentages *wpv\_nacl*, uncertainties *error*, and an initial guess of 5.6, and then plot the fit:

```
>> conds=sd_nacl2siemens(wpv_nacl);
>> bestfit=crossoverfit(s, conds, fxos, error, [5.6])
>> s=setfitChars(s,bestfit)
>> plot_cc(s,10^-3,10^-1)
>> hold on
>> loglog(conds,fxos,'.')
```

Unfortunately, there's no good way to plot error bars on log-log plots in MATLAB.

### B. Complete code

File: chisq.m

```
1 function x= chisq(changeparams, suspension, conductivities, fxos,stdevs)
2 %chisq is used by fminsearch to calculate what the error is for a given
3 %suspension.
4
5 % Creates a new suspension, identical to "suspension", but with the new
6 % parameters changeparams.
7 s = setfitChars(suspension,changeparams);
8
9 %Find the predicted data points, so that they can be compared with the
10 %experimental ones.
11 for i = 1:length(conductivities)
12     s=setConductivity(s,conductivities(i));
13     fxos_predicted(i)=crossover(s,5,.001,10^9); %Get the crossover frequency.
14         % 5,.001, and 10^9 are just values that seemed to optimize
15         % the search.
16 end;
17
18 %Find the error with the standard chi squared formula
19 x=sum((fxos-fxos_predicted').^2./stdevs.^2)
20
```

File: crossoverfit.m

```
1 function vals = crossoverfit(suspension, conductivities, fxos, stdevs, ...
2                               changeparams)
3 % function vals = crossoverfit(suspension, conductivities, fxos, stdevs,
4 %                               changeparams)
5 %
6 % crossoverfit(...) is a chi-sq minimization function.
7 % Suspension is the suspension object to be fit. Conductivities and fxos
8 % are the empirical data to be fit, and stdevs is the uncertainties in those
9 % points. Changeparams
10 % are the parameters to be changed. (Perhaps, internal conductivity,
11 % etc.) If changing which parameters will be fitted, code must be
12 % modified in setfitChars.m
13 %
14 %
15 % The [] means no options... it could be used to set which fitting
16 % algorithm to be used, or to set accuracy, or any number of options (see
17 % matlab documentation on fminsearch)
18 % @chisq identifies the chisq function as the way to determine what the
19 % error is.
```

```

20 [vals, chi_sq] = fminsearch(@chisq, changeparams, [], suspension, ...
21                                     conductivities, fxos, stdevs);
22
23 sprintf('Chisquared per Degree of Freedom was %0.3g\n Values were:'...
24     ,chi_sq/(length(fxos)-1))
25
26 changeparams
27 vals
28

```

File: plot\_cc.m

```

1 function plot_cc(susp, sigmaMin, sigmaMax)
2 % plot_cc(susp, sigmaMin, sigmaMax)
3 % Plots the crossover frequency as a function of medium conductivity.
4 % susp is a Suspension object, which contains a particle object and a
5 % medium object.
6
7 resolution = 200; % How many conductivity values to plot.
8 crossovers = zeros(resolution);
9 condDomain=logspace(log(sigmaMin)/log(10),log(sigmaMax)/log(10),resolution);
10 for i = 1:resolution
11     susp=setConductivity(susp,condDomain(i));
12     crossovers(i)=crossover(susp,5,.001,10^9); %Get the crossover frequency.
13 end;
14 %figure;
15 loglog(condDomain,crossovers);
16 xlabel('Conductivity (Sm^-^1)');
17 ylabel('Crossover frequency (Hz)');

```

File: salt2siemens.m

```

1 function siemens = salt2siemens(WpVnacl)
2 %function siemens = salt2siemens(WpVnacl)
3 % Given a weight/volume percentage (e.g., .9 for .9w/v% NaCl),
4 % salt2siemens returns the conductivity (interpolated from a data table.)
5 % Concentration must be between 0 and 2 (0 and 2% w/v).
6
7
8 % data table, taken from
9 % http://global.horiba.com/story_e/conductivity/conductivity_03.htm
10
11 salt = [0.1000    0.2000    0.3000    0.4000    0.5000    ...
12      0.6000    0.7000    0.8000    0.9000    1.0000    ...
13      1.1 1.2 1.3 1.4 1.5 1.6 1.7 1.8 1.9 2;
14      0.2000    0.3900    0.5700    0.7500    0.9200    ...
15      1.0900    1.2600    1.4300    1.6000    1.7600    1.92 ...
16      2.08 2.24 2.40 2.56 2.71 2.86 3.01 3.16 3.3];
17
18 siemens = spline(salt(:,1), salt(:,2), WpVnacl);

```

File: sd\_nacl2siemens.m

```

1 function siemens = sd_nacl2siemens(WpVnacl)
2 %function siemens = salt2siemens(WpVnacl)
3 % Given a weight/volume percentage (e.g., .9 for .9w/v% NaCl), (NaCl
4 % dissolved in a 8.5% sucrose, .3%dextrose w/v solution)
5 % sd_nacl2siemens returns the conductivity (interpolated from a data table.)
6 % Concentration should be between 0 and 1 (0 and 1% w/v) for best accuracy.
7
8 % Based on data taken on July 15, 2004 by Rob Chambers
9
10 siemens = polyval([1527.3    2.4],WpVnacl)/1000 %Result of a linear regression.

```

File: @fragment/e\_star.m

```

1 function e = e_star(s,w)
2 % e_star(s,w) e_star returns the complex permittivity of the particle.
3 % This approximates the fragment as a small dielectric sphere, with a
4 % conductance that's probably due mostly to the surface conductance of the
5 % double layer.
6

```

```

7 j=sqrt(-1);
8 e = s.e_r*8.85418782*10^-12 - j*s.sigma./w;

```

File: @fragment/fragment.m

```

1 function j = fragment(varargin)
2 % FRAGMENT class constructor, approximates a fragment as a small sphere. It
3 % probably won't be accurate, but should give us an idea of the trends we
4 % can expect from fragments.
5
6 %no arguments
7
8 % If no arguments are given, we'll fill it with some arbitrary values.
9 if nargin==0
10    j = fragment('Default Cell Fragment',... % Some identifying name.
11      1*10^-6,... % Radius of fragment [m]
12      5.6,... % Fragment permittivity [dimensionless]
13      .3) % surface conductivity (This will take into
14          %account the surface conductance due to the
15          % double layer. I have *no* idea what a realistic
16          % value is.)
17
18
19 % class argument
20 elseif isa(varargin, 'fragment');
21    j = varargin;
22
23 %normal constructor
24 elseif nargin==4
25    % Assign the values.
26    j.name = varargin{1}; % Some identifying name.
27    j.r = varargin{2}; % Cell radius.
28    j.e_r= varargin{3}; % Relative permittivity
29    j.sigma= varargin{4}; % conductivity
30    j = class(j, 'fragment'); % Defines this object as a fragment.
31 else
32    error('Wrong number of input arguments')
33 end;
34

```

File: @jurkat/e\_star.m

```

1 function e = e_star(s,w)
2 % e_star(s,w) e_star returns the complex permittivity of the particle.
3 % This is a SINGLE SHELL model (the single shell is the plasma membrane,
4 % which encloses the cytoplasm.)
5 %
6 % A good reference is
7 % Wang, X-B., Huang, Y., Gascoyne, P.R.C., Becker, F.F., Hlzel,
8 % R., and Pethig, R. "Changes in Friend murine erythroleukaemia cell
9 % membranes during induced differentiation determined by electrorotation."
10 % Biochim. Biophys. Acta, 1193:330-344, 1994.
11 % or
12 % Huang, Y., Wang, X-B., Gascoyne, P.R.C., Becker, F.F., "Membrane
13 % dielectric responses of human T-lymphocytes following mitogenic
14 % stimulation." Biochimica Et Biophysica ACTA, 1417: 51-62, 1999.
15 %
16 % The equations are explained herein.
17
18 % Permittivity of free space... we need this, since it's easy
19 % to define materials' relative permittivity.
20 e0 = 8.85418782*10^-12;
21
22
23 e_m = s.e_r_mem*e0 - j*s.sigma_mem./w; % This is the (frequency dependent) complex
24 % permittivity of the membrane.
25
26 e_int = s.e_r_int*e0 - j*s.sigma_int./w; % This is the (frequency dependent) complex
27 % permittivity of the cytoplasm.
28 r=s.r;
29 d=s.d;

```

```

30 % e_star is the effective complex permittivity of the cell as a whole.
31
32 % Now, here we have a discrepancy. Huang uses the term (r/(r-d))^3, while
33 % Wang uses ((r+d)/r)^3. It appears that the discrepancy is over what the
34 % cell radius represents (center to outside of cytoplasm, or to outside of
35 % membrane?) We'll assume it's to the outside of the membrane, as Huang
36 % did. It shouldn't make a big difference either way.
37
38 e= e_m .* ((r/(r-d))^3 + 2*((e_int - e_m)./(e_int+2*e_m))./((r/(r-d))^3 ...
39 - ((e_int - e_m)./(e_int+2*e_m)));

```

File: @jurkat/setfitChars.m

```

1 function j = setfitChars(p,chars)
2 % setFitchars(p, chars) passes those characteristics (varargin) onto the
3 % jurkat particle p.
4 % If different parameters need to be changed, then the code in this file
5 % must be reordered.
6 j=p;
7 j.name = 'Temporary fitting particle.';
8
9 % These are the parameters that will be fit.
10 j.e_r_mem= chars(1); % Relative membrane permittivity default 5.6
11
12 % These parameters are known well enough to not be fit, or are pointless to
13 % fit because the error is not sensitive to them.
14 %j.sigma_int= chars(1); % Cytoplasmic conductivity default .7
15 %j.e_r_int= chars(2); % Cytoplasmic relative permittivity default 65
16 %j.sigma_mem= varargin{5}; % Membrane conductivity
17 %j.r = varargin{2}; % Cell radius.
18 %j.d = varargin{3}; % Cell membrane thickness.

```

File: @medium/e\_star.m

```

1 function e = e_star(s,w)
2 % e_star(s,w) e_star returns the complex permittivity of the medium.
3 e = s.e_r*8.85418782*10^-12 - j*s.sigma./w;

```

File: @medium/medium.m

```

1 function m = medium(varargin)
2 % medium(varargin)
3 % MEDIUM class constructor
4 % IMPORTANT: Syntax: medium('Medium Name', e_r [dimless], sigma [S/m]);
5
6 %no arguments
7 if nargin==0
8     m=medium('Default 10mS/m Water', 78, .01);
9     % Assign default values here. Permittivity of water is 78, 10mS/m =>
10    % .01S/m.
11
12 % class argument
13 elseif isa(varargin, 'medium')
14     m = varargin;
15
16 %normal constructor
17 elseif nargin==3
18     % Assign the values.
19     m.name = varargin{1}; % Some identifying name.
20     m.e_r = varargin{2}; % Relative permittivity.
21     m.sigma = varargin{3}; % Conductivity.
22     m = class(m, 'medium');
23 else
24     error('Wrong number of input arguments')
25 end;
26

```

File: @medium/setConductivity.m

```

1 function m=setConductivity(m, newSigma)
2 % Sets the conductivity of the medium to be newSigma.
3 m.sigma = newSigma;

```

## File: @suspension/crossover.m

```

1 function fout = crossover(s,n,FMin,FMax);
2 % crossover(s,n,FMin,FMax) is a recursive function that returns the crossover
3 % frequency for a given suspension.
4 % It searches for the frequency between FMin and FMax. N decreases as it
5 % recurses. The N with which the function is called determines the
6 % accuracy, because it sets the number of recursions.
7
8 % The function increases the range if the crossover frequency is not found.
9 % The answers become good within about .1% after around 4 iterations.
10
11 f=logspace(log(FMin)/log(10),log(FMax)/log(10),50);
12 w=2*pi*f; %Need radians.
13 output=real(K(s,w)); %We only care about the real parts.
14
15 % standard zero-crossing algorithm.
16 pn=sign(output(1)); % (Which sign do we start off with?)
17 for i = 1:50
18     if sign(output(i)) ~= pn
19         break;
20     end;
21 end;
22
23 if n>1
24     if i==50 % We're too low, increase the max. range
25         fout=crossover(s,n-1,FMin,f(i)*10^4);
26     else
27         fout=crossover(s,n-1,.98*f(i-1),1.02*f(i));
28     end;
29 else
30     if i==50 % it doesn't exist.
31         fout = .01; % Assign an arbitrary value so matlab doesn't freak.
32     else
33         fout = f(i); %We found it; return the frequency.
34     end
35 end;
36
37
38
39

```

## File: @suspension/getMedium.m

```

1 function g = getMedium(s) %Annoyingly, this is necessary
2 % to access variables.
3 g = s.medium;

```

## File: @suspension/getName.m

```

1 function n = getName(s)
2 % getName(s) returns a string identifying the suspension s.
3 % This could return any name identifying the cell suspension.
4 % We'll just reutrn the variable 'name'. To really do it right, it would
5 % return the types of the particle and medium, and maybe some of their
6 % parameters.
7
8 n = s.name;

```

## File: @suspension/getParticle.m

```

1 function g = getParticle(s)
2 %Annoyingly, this is necessary to access variables. It makes no sense; it's
3 %just a Matlab thing.
4 g = s.particle;

```

## File: @suspension/K.m

```

1 function k=K(s,w);
2 % function k=K(s,w)
3 % Returns the (complex) Clausius-Mossotti factor for a given suspension.
4 % This works for spherical particles in homogeneous medium. The particle
5 % objects are responsible for providing their own implementation of

```

```

6 % e_star, depending on what model they're based on.
7
8 em=e_star(s.medium,w); % complex permittivity of medium
9
10 ep=e_star(s.particle,w); % complex permittivity of particle
11
12 k=(ep-em)./(ep+2*em); % k = clausius mossotti factor

```

File: @suspension/plotK.m

```

1 function plotK(s,mag1,mag2);
2 % function plotK(s,mag1,mag2);
3 % Plot a semilog plot of the Clausius-Mossotti factor for a suspension,
4 % from frequencies 10^mag1 to 10^mag2.
5 f=logspace(mag1,mag2,1000);
6 w=2*pi*f; % we need radians, not Hz.
7 output=real(K(s,w));
8 semilogx(f,output);
9 title(strcat('Real Part of Clausius Mossotti vs. Frequency for ', getName(s)));
10 xlabel('frequency (Hz)');
11 ylabel('Re[f(\omega)]');

```

File: @suspension/setConductivity.m

```

1 function s=setConductivity(s, newSigma)
2 % Sets the conductivity of the suspension to be newSigma.
3 % this is terribly awkward, but it's the only way I can find to do this in
4 % MatLab.
5 s.medium=setConductivity(s.medium,newSigma);

```

File: @suspension/setfitChars.m

```

1 function susp = setfitChars(s,chars)
2 % setFitchars(s, chars) passes those characteristics chars onto the
3 % particle in suspension s.
4 susp = suspension('Temporary fitting suspension', ...
5 setfitChars(getParticle(s), chars),getMedium(s));

```

File: @suspension/suspension.m

```

1 function s = suspension(varargin)
2 % SUSPENSION class constructor
3 % IMPORTANT: Syntax: suspension('Suspension Name', suspended particle, medium);
4
5 %no arguments
6 if nargin==0
7     j = jurkat;
8     m = medium;
9     s = suspension('Jurkats in Default water.', j, m);
10    % Assign default values here.
11
12 % class argument
13 elseif isa(varargin, 'suspension')
14     s = varargin;
15
16 %normal constructor
17 elseif nargin==3
18     % Assign the values.
19     s.name = varargin{1};
20     s.particle = varargin{2};
21     s.medium = varargin{3};
22     s = class(s, 'suspension');
23 else
24     error('Wrong number of input arguments');
25 end;
26

```

**APPENDIX V**  
**FRAGMENT CREATION AND QUANTIFICATION PROTOCOL**

*A. Creation*

For ten one-mL samples. Amounts of PBS can be scaled to change cell concentration. The protocol is rather flexible. Aggregation becomes a problem at cell concentrations  $> 10^6$  cells/mL.

- 1) Centrifuge two 5-mL portions of cell culture, 7 minutes, 1000 RPM.
- 2) For each 5-mL portion: Pour off supernatant. Add 5mL PBS and, without disturbing cell pellet, pour off. Add 5mL PBS and gently pipette up and down.
- 3) Centrifuge another 7 minutes, 1000 RPM.
- 4) Pour of supernatant, resuspend each in 5mL PBS.
- 5) Separate into 10 1-mL aliquots using 1.5mL Micro Tubes.
- 6) For each freeze/thaw cycle:
  - Place in -80°C freezer, leave 25 minutes.
  - Remove, thaw in 37°C water bath 10 minutes.
- 7) Avoid unnecessary vortexing, which *may* contribute to aggregation.

*B. Quantification*

- 1) Start machine and CellQuest software according to the posted instructions.
- 2) Set data to be acquired for 30 seconds, set # of events to an arbitrarily high number.
- 3) Set all channels to log, forward scatter to E-1, side scatter amplification to 320, and forward scatter threshold to 10.
- 4) On a new worksheet, draw a dotplot (FSC vs. SSC)
- 5) Display region statistics, set display mode to “cumulative.”
- 6) For each sample:
  - Vortex slightly at medium speed.
  - Pour  $\approx 500\mu\text{L}$  of sample into a Falcon 2054 flow tube.
  - Load into machine, set speed to “low,” set mode to “run.”
  - In CellQuest, press “acquire.”
  - If first sample, draw gates around Cells and Debris.
  - Record desired measurements, such as # Total events, # Debris events, and # Cell events.

## ACKNOWLEDGMENT

Thanks to Prof. Allison Hubel, my faculty advisor; and to Katie Fleming, my graduate student mentor; and to the rest of the Hubel lab.

Also, thanks to Sue Mantell and Jane Davidson for organizing the REU program, and to Paul Champoux at the UMN Immunology Center for assisting with the flow cytometry.

## REFERENCES

- [1] Y. Huang, J. Yang, X.-B. Wang, F. F. Becker, and P. R. C. Gascoyne, "The removal of human breast cancer cells from hematopoietic cd34+ stem cells by dielectrophoretic field-flow-fractionation," *Journal of Hematology and Stem Cell Research*, vol. 8, pp. 481–490, 1999.
- [2] P. Gascoyne, C. Mahidol, M. Ruchirawat, J. Satayavivad, P. Watcharasit, and F. F. Becker, "Microsample preparation by dielectrophoresis: isolation of malaria," *Lab on a Chip*, vol. 2, pp. 70–75, 2002.
- [3] D. Holmes, N. G. Green, and H. Morgan, "Microdevices for dielectrophoretic flow-through cell separation," *IEEE Engineering in Medicine and Biology Magazine*, pp. 85–90, Nov/Dec 2003.
- [4] G. D. Gasperis, J. Yang, F. F. Becker, P. R. C. Gascoyne, and X.-B. Wang, "Microfluidic cell separation by 2-dimensional dielectrophoresis," *Biomedical Microdevices*, vol. 2, no. 1, pp. 41–49, 1999.
- [5] J. Yang, Y. Huang, X.-B. Wang, F. F. Becker, and P. R. C. Gascoyne, "Differential analysis of human leukocytes by dielectrophoretic field-flow-fractionation," *Biophysical Journal*, vol. 78, pp. 2680–2689, May 2000.
- [6] B. H. Lapizco-Encinas, B. A. Simmons, E. B. Cummings, and Y. Fintschenko, "Dielectrophoretic concentration and separation of live and dead bacteria in an array of insulators," *Analytical Chemistry*, vol. 76, pp. 1571–1579, 2004.
- [7] Y. Huang, R. Holzel, R. Pethig, and X.-B. Wang, "Differences in the ac electrodynamics of viable and non-viable yeast cells determined through combined dielectrophoresis and electrorotation studies," *Physics in Medicine and Biology*, vol. 37, no. 7, pp. 1499–1517, 1992.
- [8] P. R. C. Gascoyne and J. Vykkoukal, "Particle separation by dielectrophoresis," *Electrophoresis*, vol. 23, pp. 1973–1983, 2002.
- [9] X. Wang, Y. Huang, P. Gascoyne, F. Becker, R. Holzel, and R. Pethig, "Changes in friend murine erythroleukaemia cell membranes during induced differentiation determined by electrorotation," *Biochimica et Biophysica Acta-Biomembranes*, vol. 1193, no. 2, pp. 330–344, Aug 1994.
- [10] Y. Huang, X. Wang, P. Gascoyne, and F. Becker, "Membrane dielectric responses of human t-lymphocytes following mitogenic stimulation," *Biochimica et Biophysica Acta-Biomembranes*, vol. 1417, no. 1, pp. 51–62, Feb 1999.
- [11] M. P. Hughes, *Nanoelectromechanics in Engineering and Biology*. Boca Raton: CRC Press, 2003.
- [12] J. Yang, Y. Huang, X.-B. Wang, F. F. Becker, and P. R. C. Gascoyne, "Cell separation on microfabricated electrodes using dielectrophoretic/gravitational field-flow fractionation," *Analytical Chemistry*, vol. 71, no. 5, pp. 911–918, Mar 1999.
- [13] H. Morgan, A. G. Izquierdo, D. Bakewell, N. G. Green, and A. Ramos, "The dielectrophoretic and travelling wave forces generated by interdigitated electrode arrays: analytical solutions using fourier series," *Journal of Physics D: Applied Physics*, vol. 34, pp. 1553–1561, 2001.
- [14] C.-F. Chou, J. O. Tegenfeldt, O. Bakajin, S. S. Chan, E. C. Cox, N. Darnton, T. Duke, and R. H. Austin, "Electrodeless dielectrophoresis of single- and double-stranded dna," *Biophysical Journal*, vol. 83, pp. 2170–2179, October 2002.
- [15] C.-F. Chou and F. Zenhausern, "Electrodeless dielectrophoresis for micro total analysis systems," *IEEE Engineering in Medicine and Biology Magazine*, pp. 62–67, November/December 2003.
- [16] S. S. Sekhon, "Conductivity behaviour of polymer gel electrolytes," *Bulletin of Materials Science*, vol. 26, no. 3, pp. 321–328, April 2003.
- [17] *Smithsonian Physical Tables*, 9th ed., Knovel, 2003, p. 397.
- [18] D. B. Murphy, *Fundamentals of light microscopy and electronic imaging*. New York: Wiley-Liss, 2001.
- [19] J. R. D. Wet, K. V. Wood, M. DeLuca, D. R. Helinski, and S. Subramani, "Firefly luciferase gene: Structure and expression in mammalian cells," *Molecular and Cellular Biology*, vol. 7, no. 2, pp. 725–737, Feb 1987.
- [20] D. A. Vessey, "Isolation and preliminary characterization of the medium-chain fatty acid: Coa ligas responsible for activation of short- and medium-chain fatty acids in colonic mucosa from swine," *Digestive Diseases and Sciences*, vol. 46, no. 2, pp. 438–442, Feb 2001.
- [21] L.-P. Broudiscou, H. Geissler, and A. Broudiscou, "Estimation of the growth rate of mixed ruminal bacteria from short-term dna radiolabeling," *Anaerobe*, vol. 4, pp. 145–152, 1998.
- [22] J. S. Andersen, C. J. Wilkinson, T. Mayor, P. Mortensen, E. A. Nigg, and M. Mann, "Proteomic characterization of the human centrosome by protein correlation profiling," *Nature*, vol. 246, pp. 573–574, 2003.
- [23] V. Catts, M. Farnsworth, M. Haber, M. Norris, L. Lutze-Mann, and R. Locke, "High level resistance to glucocorticoids, associated with a dysfunctional glucocorticoid receptor, in childhood acute lymphoblastic leukemia cells selected for methotrexate resistance," *Leukemia*, vol. 15, pp. 929–935, 2001.
- [24] G. G. Oakley, L. I. Loberg, J. Yao, M. A. Risinger, R. L. Lunker, M. Zernik-Kobak, K. K. Khanna, M. F. Lavin, M. P. Carty, and K. Dixon, "Uv-induced hyperphosphorylation of replication protein a depends on dna replication and expression of atm protein," *Molecular Biology of the Cell*, vol. 12, pp. 1199–1213, May 2001.
- [25] B. Cuevas, Y. Lu, S. Watt, R. Kumar, J. Zhang, K. A. Siminovitch, and G. B. Mills, "Shp-1 regulates lck-induced phosphatidylinositol 3-kinase phosphorylation and activity," *Journal of Biological Chemistry*, vol. 274, no. 39, pp. 27 583–27 589, September 1999.
- [26] D. C. S. Hang, M. Hahne, M. Schroeter, K. Frel, A. Fontano, A. Vil-lunger, K. Newton, J. Tschoopp, and A. Strasser, "Activation of fas by fasl induces apoptosis by a mechanism that cannot be blocked by bcl-2 or bcl-xL," *PNAS*, vol. 96, no. 26, pp. 14 871–14 876, December 1999.
- [27] C. Prinz, J. O. Tegenfeldt, R. H. Austin, E. C. Cox, and J. C. Sturm, "Bacterial chromosome extraction and isolation," *Lab on a Chip*, vol. 2, pp. 207–212, 2002.
- [28] J. R. Mitchell, E. Wood, and K. Collins, "A telomerase component is defective in the human disease dyskeratosis congenita," *Nature*, vol. 402, pp. 551–555, December 1999.
- [29] O. Héroult, C. Binet, A. Rico, M. Degenne, M.-C. Bernard, M. Chassaigne, and L. Sensebe, "Evaluation of performance of white blood cell reduction filters: An original flow cytometric method for detection and quantification of cell-derived membrane fragments," *Cytometry*, vol. 45, pp. 277–284, 2001.
- [30] T. B. Jones, *Electromechanics of Particles*. New York: Cambridge UP, 1995.
- [31] V. L. Sukhorukov, M. Kurschner, S. Dilksy, T. Lisek, B. Wagner, W. A. Schenck, R. Benz, and U. Zimmermann, "Phloretin-Induced Changes of Lipophilic Ion Transport across the Plasma Membrane of Mammalian Cells," *Biophys. J.*, vol. 81, no. 2, pp. 1006–1013, 2001. [Online]. Available: <http://www.biophysj.org/cgi/content/abstract/81/2/1006>
- [32] R. Pethig, V. Bressler, C. Carswell-Crompton, Y. Chen, L. Foster-Haje, M. E. Garca-Ojeda, R. S. Lee, G. M. Lock, M. S. Talary, and K. M. Tate, "Dielectrophoretic studies of the activation of human t lymphocytes using a newly developed cell profiling system," *Electrophoresis*, vol. 23, no. 13, pp. 2057–2063, July 2002.
- [33] R. Pethig and D. B. Kell, "The passive electrical properties of biological systems: their significance in physiology, biophysics and biotechnology," *Physics in Medicine and Biology*, vol. 32, no. 8, pp. 933–970, 1987.
- [34] J. Gimsa and D. WAchner, "A unified resistor-capacitor model for impedance, dielectrophoresis, electrorotation, and induced transmembrane potential," *Biophysical Journal*, vol. 75, no. 2, pp. 1107–1116, August 1998.
- [35] M. Kürschner, K. Nielsen, J. R. von Langen, W. A. Schenck, U. Zimmermann, and V. L. Sukhorukov, "Effect of fluorine substitution on the interaction of lipophilic ions with the plasma membrane of mammalian cells," *Biophysical Journal*, vol. 79, no. 3, pp. 1490–1497, 2000.
- [36] H. Morgan, M. P. Hughes, and N. G. Green, "Separation of submicron bioparticles by dielectrophoresis," *Biophysical Journal*, vol. 77, no. 1, pp. 516–525, July 1999.
- [37] A. Docoslis, N. Kalogerakis, L. A. Behie, and K. V. I. S. Kaler, "A novel dielectrophoresis-based device for the selective retention of viable cells in culture media," *Biotechnology and Bioengineering*, vol. 53, no. 3, pp. 239–250, 1997.
- [38] A. Docoslis, N. Kalogerakis, and L. A. Behie, "Dielectrophoretic forces can be safely used to retain viable cells in perfusion cultures of animal cells," *Cytotechnology*, vol. 30, pp. 133–142, 1999.
- [39] T. B. Jones, "Liquid dielectrophoresis on the microscale," *Journal of Electrostatics*, vol. 51, no. 52, pp. 290–299, 2001.
- [40] P. K. Wong, T.-H. Wang, J. H. Deval, and C.-M. Ho, "Electrokinetics in micro devices for biotechnology applications," *IEEE/ASME Transaction on Mechantronics*, pp. 1–12, 2003.